

Experimental Study of Combustion Characteristics of Bituminous Char Derived under Mild Pyrolysis Conditions

Chunmei Shen,^{†,‡} Weigang Lin,[‡] Shaohua Wu,^{*,†} Xiaobo Tong,[‡] and Wenli Song[‡]

[†]School of Energy Science and Engineering, Harbin Institute of Technology, Harbin, 150001, People's Republic of China, and

[‡]State Key Laboratory of Multi-phase Complex System, The Institute of Process Engineering, Chinese Academy of Sciences, Beijing, 100190, People's Republic of China

Received April 7, 2009. Revised Manuscript Received July 31, 2009

The combustion characteristics of chars derived from a bituminous coal (Datung, also denoted as DT) at different pyrolysis temperatures were studied via simultaneous thermal analysis (STA). The chars were obtained at pyrolysis temperatures of 550, 650, 750, and 850 °C. The carbon structure of chars and the parent coal were characterized using X-ray diffraction. Pore structures of chars and parent coal were measured by nitrogen adsorption. Based on the thermogravimetric analysis results, the ignition behavior and reactivity of the chars and the parent coal, as well as those of Yangquan (YQ) anthracite, were compared. The ignition temperature (T_i) and weighted mean apparent activation energy (E_m) were obtained and used to evaluate reactivity. The results show that the ignition type of the bituminous parent coal and chars derived at 550, 650, and 750 °C is predominately hetero-homogeneous, whereas that of char derived at 850 °C and the YQ anthracite is heterogeneous. Thermal deactivation was observed under the pyrolysis conditions in this work. The reactivity of all chars is lower than that of the parent coal but higher than that of Yangquan anthracite. Moreover, the char that was derived at 650 °C has the highest reactivity among all chars. Carbon structure ordering contributes more to the thermal deactivation at high temperatures than at low temperatures. Changes in pore structure and material composition affect the reactivity for chars derived from both low and high temperatures.

1. Introduction

Coal is the major energy resource in China, which accounts for about three-quarters of the total energy consumption. Such an energy profile is caused by the distribution of the energy reserves, especially the fossil fuel reserves in China: this country is abundant in coal and limited in natural gas and petroleum. Thus, reasonable utilization of coal is a challenge. Coal is a mixture of organic compounds and a small amount of inorganic ingredients. During the thermal conversion, the volatile matters in coal will first release, which are mainly composed of CO, CO₂, and hydrocarbons. The resources of high-volatile coal (bituminous coal and lignite) in China comprise up to 85% of the total coal reserves. The high-volatile coals may be utilized to extract aromatic hydrocarbons such as tar as liquid products under mild conditions before being further combusted for power generation by a hybrid process. The so-called “coal topping” process is such a process, which was proposed at the Institute of Process Engineering, Chinese Academy of Sciences (IPE, CAS).¹ The system has been realized in a circulating fluidized bed

(CFB) system.^{2–4} In the system, the return leg acts as a pyrolyzer, from which volatile matters are released by mixing coal with a hot recirculating solid in the system. The remaining char goes back to the combustor (riser), together with the recirculating solid. The released volatile matters are separated with solid particles and quenched to obtain liquid and gaseous products. Such processes may be competitive technically and economically. However, the system presently can only be applied in a CFB system, which limits its application to wider consumers of coal. By considering the fact that the majority of coal consumed in the power industry is burned in pulverized mode, the idea of combining the coal topping process with a pulverized coal boiler was proposed, from which the pulverized coal is pyrolyzed first to obtain a certain amount of liquid and gaseous products. The char will be injected to the burners and combusted in the pulverized coal furnace. However, the combustion behaviors of the char will govern the performance of the pulverized burner and furnace when a pulverized coal combustor is combined with the coal topping process. Unlike the CFB system, pulverized coal combustors are more sensitive to the type of coal.⁵ Thus, it is important to obtain a basic knowledge of how the pyrolysis conditions affect the char combustion characteristics, such as ignition temperature and combustion reactivity.

*To whom correspondence should be addressed. Tel.: +86-451-8641-2628. Fax: +86-451-8641-2528. E-mail address: wush@hit.edu.cn.

(1) Kwauk, M. S. Coal Topping Process. In *Selected Papers of the 9th Member Forum of Academia Sinica*; Academic Press: Beijing, 1998; pp 202–204.

(2) Wang, J. G.; Lu, X. S.; Yao, J. Z.; Lin, W. G.; Cui, L. J. Experimental Study of Coal Topping Process in a Downer Reactor. *Ind. Eng. Chem. Res.* **2005**, *44* (3), 463–470.

(3) Yao, J. Z.; Wang, X. Q.; Lin, W. G., Coal Topping in a Fluidized Bed System. In *The 16th International Conference on Fluidized Bed Combustion*, Reno, NV, 2001.

(4) Wang, J. G.; Wang, X. Q.; Yao, J. Z., Coal Topping Process and its Preliminary Experiments. In *Proceedings of the 7th China–Japan Symposium on Coal and Chemistry*, 2001; pp 185–188.

(5) Li, Z. Q.; Yang, L. B.; Qiu, P. H.; Sun, R.; Chen, Z. C.; Sun, S. Z. Experimental study of the combustion efficiency and formation of NO_x in an industrial pulverized coal combustor. *Int. J. Energy Res.* **2004**, *28* (6), 511–520.

During pulverized coal combustion, combustion can be divided into two stages: (i) volatile release and combustion and (ii) char combustion. Devolatilization and volatile combustion is fast, compared to the char combustion. Thus, the characteristics of the char combustion play an important role in burnout processes. Extensive investigations have been conducted to determine the combustion reactivity of chars derived from high-temperature pyrolysis.^{6–13} With the development of coal poly-generation technologies, the reactivity of chars derived under relevant conditions was studied.^{14–16} The previous studies show that char reactivity is very sensitive to the pyrolysis conditions. In addition, chars derived from different pyrolysis conditions have significant differences, in physical and chemical properties.^{9–12} The pore structure evolution and the structural ordering of the carbon on a molecular level occur during pyrolysis. These two factors have a significant effect on the reactivity of the chars.^{6,8,9,12,13} Our previous work on the coal topping process was mainly focused on flash pyrolysis mechanisms of coal and the product distribution under different pyrolysis conditions.^{2–4,17–19} The combustion characteristics of the chars derived from the coal topping process have yet to be studied.

The object of this work is to study the ignition and combustion characteristics of chars derived from the coal topping process under different pyrolysis temperatures to answer the following questions:

- (1) What is the difference between the parent coal and the char in combustion characteristics?
- (2) What are the reasons that cause such differences?

(6) Lu, L. M.; Kong, C. H.; Sahajwalla, V.; Harris, D. Char structural ordering during pyrolysis and combustion and its influence on char reactivity. *Fuel* **2002**, *81* (9), 1215–1225.

(7) Alonso, M. J. G.; Borrego, A. G.; Alvarez, D.; Menendez, R. A reactivity study of chars obtained at different temperatures in relation to their petrographic characteristics. *Fuel Process. Technol.* **2001**, *69* (3), 257–272.

(8) Cai, H. Y.; J., G. A.; Chatzakis, I. N.; et al. Combustion Reactivity and Morphological Change in Coal Chars: Effect of Pyrolysis Temperature, Heating Rate and Pressure. *Fuel* **1996**, *75* (1), 15–24.

(9) Wells, W. F.; Soot, L. D. Relation between reactivity and structure for coals and chars. *Fuel* **1991**, *70*, 454–458.

(10) Gale, T. K.; Bartholomew, C. H.; Fletcher, T. H. Effect of pyrolysis heating rate on intrinsic reactivities of coal chars. *Energy Fuels* **1996**, *10*, 766–775.

(11) Shim, H.; Hurt, R. Thermal annealing of chars from diverse organic precursors under combustion-like conditions. *Energy Fuels* **2000**, *14* (2), 340–348.

(12) Russell, N. V.; Gibbins, J. R.; Williamson, J. Structural ordering in high temperature coal chars and the effect on reactivity. *Fuel* **1999**, *78*, 803–807.

(13) Best, P. E.; Solomon, P. R.; Serio, M. A.; et al. The Relationship between Char Reactivity and Physical Chemical Structural Features. *Am. Chem. Soc., Div. Fuel Chem.* **1987**, *32*, 44–51.

(14) Chen, X. P.; Gu, X. B.; Duan, Y. F.; Zhao, C. S.; Wu, X. Investigation on the combustion characteristics of semi-coke at elevated pressure. *J. Eng. Thermophys.* **2004**, *25* (2), 345–347.

(15) Sheng, H. Z.; Liu, D. F.; Wei, X. L.; Huang, N. Characteristics of semi-coke - the solid residues from coal partial gasification. *J. Combust. Sci. Technol.* **2004**, *10* (2), 187–191.

(16) Shen, S. Q.; Li, S. F.; Shi, Y. Experimental investigation on the ignition and combustion of semi-coke particles. *J. Combust. Sci. Technol.* **2000**, *6* (1), 66–69.

(17) Cui, L. J.; Song, W. L.; Zhang, J. Y.; Yao, J. Z.; Lin, W. G. Influence of the Gas and particle residence time on fast pyrolysis of lignite. *Trans. ASME* **2007**, *129*, 152–158.

(18) Cui, L. J.; Lin, W. G.; Yao, J. Z. Influences of Temperature and Coal Particle Size on the Flash Pyrolysis of Coal in a Fast-entrained Bed. *Chem. Res. Chin. Univ.* **2006**, *22* (1), 103–110.

(19) Cui, L. J.; Yao, J. Z.; Lin, W. G.; Zhang, Z., Product distribution from flash pyrolysis of coal in a fast fluidized bed. In *Proceedings of the 17th International Conference on Fluidized Bed Combustion*, Jacksonville, FL, May 18–21, 2003. (CD-ROM)

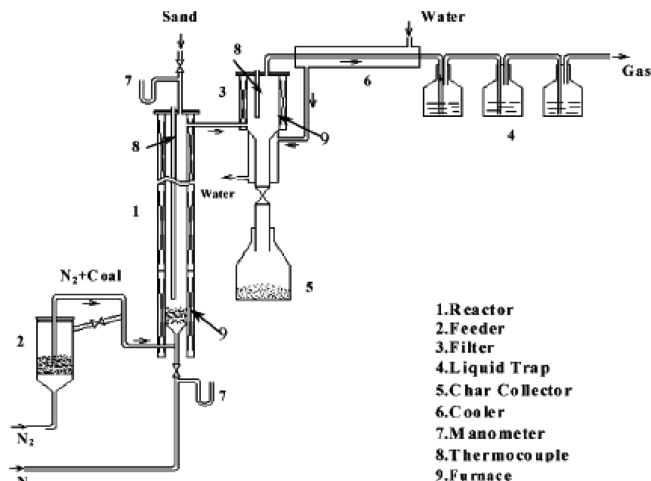


Figure 1. Schematic drawing of the pyrolysis apparatus.

(3) Is it possible for chars to have higher reactivity than anthracite, which may provide an opportunity for the coal topping process to combine with an anthracite-fired pulverized-coal combustor.

The combustion of fuels is normally characterized by the ignition temperature and the combustion reactivity. Various experimental techniques were applied to determine the ignition temperature of coal. The coal ignition type was classified into three types: homogeneous ignition, heterogeneous ignition, and hetero-homogeneous ignition.^{20,21} In the present work, the ignition temperature of the coal and the derived chars, as well as ignition type and reactivity, are determined from the results obtained in simultaneous thermal analysis. The physical and chemical characteristics of the coal and chars, such as pore structure and carbon structure of chars, are measured and used to interpret the difference in reactivity.

2. Experimental Section

2.1. Char Preparation. Datung (DT) coal, which is a bituminous coal, was used in the present study. The coal was milled to a particle size of < 0.18 mm. The coal samples were dried at 105 °C for 4 h. A spout-entrained reactor was used to prepare the char samples by flash pyrolysis of the coal particles at various temperatures. Figure 1 shows a schematic drawing of the apparatus. The detailed description of the spout-entrained reactor has been given elsewhere.^{17,18} Quartz sand with an average particle size of 0.25 mm was used as bed material. Nitrogen was used as the fluidized gas, as well as the carrying gas to feed coal particles from the bottom of the reactor. A gas flow rate of 0.6 m³/h was chosen in such a way that only char particles were elutriated and the quartz sand particles remained in the bed. The char particles were separated by a cyclone with a metallic filter and collected in a water-cooled container below the cyclone. Chars were prepared at four pyrolysis temperatures: 550, 650, 750, and 850 °C. These chars are denoted as Char550, Char650, Char750, and Char850, respectively. The operating conditions of char preparation are summarized in Table 1. The proximate and ultimate analyses for the parent coal and derived chars are shown in Table 2.

(20) Tognotti, L.; Malotti, A.; Petarca, L.; Zanelli, S. Measurement of ignition temperature of coal particles using a thermogravimetric technique. *Combust. Sci. Technol.* **1985**, *44*, 15–28.

(21) Chen, Y.; Mori, S.; Pan, W. P. Studying the mechanisms of ignition of coal particles by TG-DTA. *Thermochim. Acta* **1996**, *275* (1), 149–158.

Table 1. Summary of Operating Conditions for Char Preparation

condition	value
flow rate of fluidizing gas	0.6 m ³ /h
flow rate of feedstock	3–4 g/min
pyrolysis pressure	atmospheric
amount of feedstock	500–600 g
pyrolysis temperatures	550, 650, 750, 850 °C

2.2. Simultaneous Thermal Analysis (STA) Test. The ignition and reactivity measurements were performed in a simultaneous thermal analyzer (Netzsch, Model STA-449C). The Datung (DT) coal and chars, obtained at four pyrolysis temperatures, were tested. For comparison, Yangquan (YQ) coal (an anthracite) was also tested. Its proximate and ultimate analyses are given in Table 2. Prior to a test, the coal or char samples were milled to a particle size of <0.074 mm and dried at 105 °C for 24 h. Experimental conditions were as follows: heating rate = 2 K/min; gas (air for combustion and N₂ for pyrolysis) flow rate = 50 cm³/min, sample weight ≈ 5 mg, and ultimate temperature = 900 °C.

2.3. Carbon Structure and Pore Structure Measurements. The carbon structure of coal and chars were characterized by X-ray diffraction (XRD) measurements. These tests were performed with an X-ray diffractometer (X'Pert MPD Pro, PANalytical, The Netherlands). The samples were scanned in a step mode with a step angle of 0.03° over a range from 10°–90°.

Pore structures of coal and chars were characterized by an automated adsorption analyzer (AUTOSORB-1MP, Quanta Chrome Corp.). The adsorption/desorption isotherms were obtained with nitrogen at 77 K in a relative pressure of 0.01–0.99. The pore size distributions were calculated from the results of desorption isotherms, based on nonlocal density functional theory (NLDFT).^{22,23}

3. Results and Discussion

3.1. Ignition Temperature. Ignition temperatures are determined using the method proposed by Tognotti et al.²⁰ The ignition temperature (T_i) is considered to be the temperature of the turning point where the TG curve during combustion and the TG curve during pyrolysis are departed rapidly.

Figure 2 presents the typical TG–temperature curves during combustion and pyrolysis. The figure shows two departing points between the combustion curve and pyrolysis curve, which are marked “A” and “B” in Figure 2, respectively. From the point A onward, the sample weight for combustion slightly increases and reaches a maximum value and then decreases gradually, while the pyrolysis curve decreases slowly. The two curves intersect at point B, from which the two curves depart rapidly. The results are different from those reported by Tognotti et al.,²⁰ in which only point B existed. In the present work, point B is defined as the ignition point, as proposed by Tognotti et al., despite the small difference of the presence of point A. Table 3 summarizes the ignition temperatures of tested coal and chars.

To reveal the reason why the sample weight increases, TG tests were performed for the dried and undried samples with an ultimate temperature of 350 °C. Figure 3 shows the typical weight loss under pyrolysis and combustion conditions, using dried and undried samples. It can be seen that the weight increase occurs under combustion conditions (with

air as the carrying gas) for both dried and undried samples, starting at ~150 °C. This phenomenon may be caused by the chemisorption of oxygen on the active sites of the fuel samples, since no weight increase is observed under pyrolysis conditions (with N₂ as the carrying gas). Such phenomena have been reported in the literature.^{24–26} Furimsky et al.²⁴ concluded that certain low-molecular-weight species, such as H₂O, were removed during the drying process. When the sample is heated in the presence of air, O₂ may be chemisorbed on the sites previously occupied by these species, leading to a weight increase in the samples. Chen²⁵ assumed that the weight increase is caused by the formation of a complex that is formed via interaction between the coal sample and oxygen.

3.2. Ignition Type. Thermogravimetry–differential scanning calorimetry (TG–DSC) curves are used to determine the ignition type of the fuel samples, which have been proposed by Chen et al.²¹ For homogeneous ignition, two exothermic peaks appear, in front of and at the back of the turning point on the DSC curve. The first peak is caused by the combustion of volatile matters and the second is caused by the combustion of the residual char. For heterogeneous ignition, only one exothermic peak appears on the DSC curve; it is caused by the burning of the coal particle. In the case of hetero-homogeneous ignition, after part of the volatile matter has been released, one exothermic peak appears on the DSC curve with a remarkable weight loss on the TG curve.

Figure 4 presents differential thermogravimetry–differential scanning calorimetry (DTG–DSC) curves for the coal and chars. From the curves in Figures 4a–d, and the definition of ignition type, it can be deduced that the ignition type of DT coal, as well as Char550, Char650, and Char750, belongs to hetero-homogeneous ignition, in which part of the volatile matter is released when ignition occurs. For Char850 (see Figure 4 e), one exothermic peak occurs on the DSC curve and the weight loss between the initial point and the ignition point is very small, which implies that the ignition type is heterogeneous ignition. This type is applied to the YQ anthracite (see Figure 4 f).

Chen et al.²¹ reported that, with the same particle size, as the coal type changes from lignite through bituminous coal to anthracite with decreasing volatile matter content, the ignition type shifts from homogeneous ignition, through hetero-homogeneous ignition, to heterogeneous ignition. In the present work, the ignition type changes from hetero-homogeneous for DT coal, Char550, Char650, and Char750 to heterogeneous for Char850 and YQ coal. The volatile matter content from the parent DT coal to chars decreases as the pyrolysis temperature increases (see Table 2); thus, the ignition type seems to be determined by the volatile matter content.

It is noticed from Figure 4 that the DSC curves do not have the same shape as that of the DTG curves. This seems to be unreasonable, because the shape of the two curves should be more or less the same. The possible reason for the difference may lie in the effect of ash on the DSC curve. Figure 5 shows

(24) Furimsky, E. Effect of H/C ratio on coal ignition. *Fuel Process. Technol.* **1988**, *19* (2), 203–210.

(25) Chen, J. Y. *Study of Ignition Process and Combustion Model of Pulverized Coal*, Thesis, Huazhong University of Science and Technology, Wuhan, PRC, 1989.

(26) Chen, H. *Study on Pore Structure and Combustion Kinetics of Char during Raw Coal Burnout*, Thesis, Huazhong University of Science and Technology, Wuhan, PRC, 1994.

(22) Ravikovitch, P. I.; Neimark, A. V., Density Functional Theory Model of Adsorption Deformation. *Langmuir* **2006**, *22*, 10864–10868.

(23) Ravikovitch, P. I.; Vishnyakov, A.; Neimark, A. V. Density functional theories and molecular simulations of adsorption and phase transitions in nanopores. *Phys. Rev.* **2001**, *64* (1), 011602.

Table 2. Proximate and Ultimate Analyses of Coals and Chars

material	Proximate Analysis (%)				Ultimate Analysis (%)			
	moisture, M_{ad}	volatile matter, V_d	ash, A_d	fixed carbon, FC_d	C_d	H_d	N_d	(S + O) _d
DT	4.70	29.44	14.01	56.55	68.30	3.60	0.72	12.19
Char550	1.68	23.46	15.03	61.51	69.18	3.12	0.74	11.93
Char650	2.02	17.97	17.1	64.93	69.74	2.58	0.72	9.86
Char750	1.66	14.01	17.3	68.96	73.80	2.57	0.77	5.55
Char850	1.12	9.02	21.7	69.81	73.02	1.60	0.68	3.53
YQ	1.11	8.2	25.85	65.95	66.7	2.41	1.13	4.96

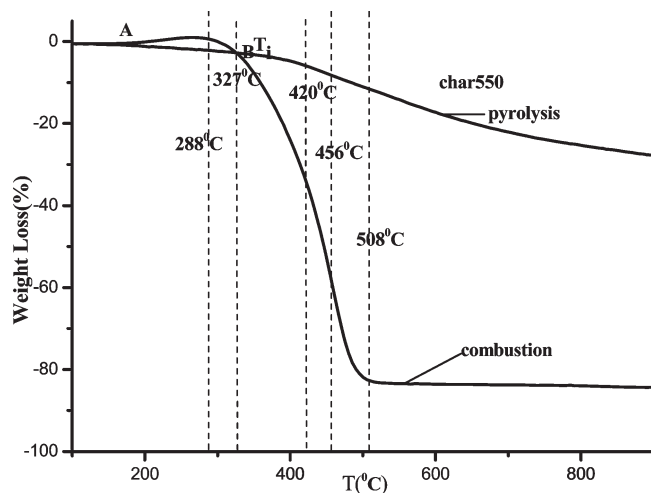


Figure 2. Typical TG combustion and TG pyrolysis curves for determination of the ignition temperature.

Table 3. Ignition Temperature of Char and Coals

sample	ignition temperature, T_i (°C)	$\Delta T_i = T_{i,char} - T_{i,DT}$ (°C)
DT	311	
Char550	327	16
Char650	328	17
Char750	341	30
Char850	354	43
YQ	430	

the TG, DTG, and DSC curves of the residual ash generated from Char550 in an air atmosphere. The DSC curve in Figure 5 reflects the thermal effect of the ash in the temperature range studied, which causes the difference between the DTG and DSC curves that is observed in Figure 4.

3.3. Reactivity. The reactivity of coal and chars in this study is expressed by the apparent kinetic parameters, which is described by a global reaction model (see eqs 1 and 2).

$$\frac{d\alpha}{dt} = k(1 - \alpha)^n \quad (1)$$

$$k = A \exp\left(\frac{-E}{RT}\right) \quad (2)$$

where k is the reaction rate constant, α the conversion of combustible materials in coal and char, n the reaction order, E the apparent activation energy, and A the pre-exponential factor.

To determine the kinetic parameters using the above equations from experimental results, various analysis

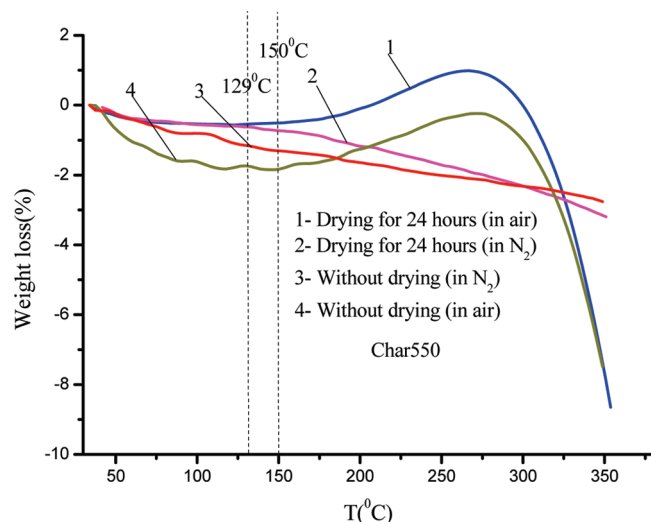


Figure 3. Plot of typical weight loss versus temperature, with an ultimate temperature of 350 °C.

methods have been proposed.²⁷ In this study, the nonisothermal analysis method²⁸ was applied.

Equation 3 can be obtained by rearranging eqs 1 and 2:

$$\ln(1 - \alpha)^{-n} \frac{d\alpha}{dt} = \ln A - \left(\frac{E}{R}\right) \left(\frac{1}{T}\right) \quad (3)$$

The values of $d\alpha/dt$ and α can be obtained directly from the TG curves. To determine the apparent kinetic parameters in eq 3, the reaction order (n) needs to be assumed. Thus, the calculated results of the left-hand side of eq 3 can be plotted against the reciprocal temperature (give in Kelvin).

The slope of the $\ln(1 - \alpha)^{-n} (d\alpha/dt)$ vs $1/T$ plot is $-E/R$. Thus, n should be a value that makes the slope negative in the applied temperature range. It was reported that the $\ln(1 - \alpha)^{-n} (d\alpha/dt)$ vs $1/T$ plots of a large number of coals are characterized by two or more regions of striking linearity, each with its own associated value of apparent activation energy.^{29–31} The present work uses the same method. The reaction order n was determined based on the following hypothesis and fulfilled to the requirements of (1) n is the same for all samples, (2) the slope of the $\ln(1 - \alpha)^{-n} (d\alpha/dt)$ vs $1/T$ plots of coals and chars are negative in the combustion temperature range, and (3) the $\ln(1 - \alpha)^{-n} (d\alpha/dt)$ vs $1/T$ plots of the coals and chars have higher linear correlation coefficient R in each region.

(29) Smith, S. E.; Neavel, R. C.; Hippo, E. J.; Miller, R. N. DTGA combustion of coals in the Exxon coal library. *Fuel* **1981**, 60 (6), 458–462.

(30) Cumming, J. W. Reactivity assessment of coals via a weighted mean activation energy. *Fuel* **1983**, 63, 1436–1440.

(31) Jiang, X. M.; Yang, H. P.; Liu, H.; Zheng, C. G.; Liu, D. C., Analysis of the effect of coal powder granularity on combustion characteristics by thermogravimetry. *Proc. CSEE* **2002**, 22 (12), 142–145, 160.

(27) Hu, R. Z.; Shi, Q. Z. *Thermal Analysis Kinetics*; Science Press: Beijing, 2001.

(28) Chen, Y.; Mori, S.; Pan, W. P. Estimating the Combustibility of Various Coals by TG-DTA. *Energy Fuels* **1995**, 9 (1), 71–74.

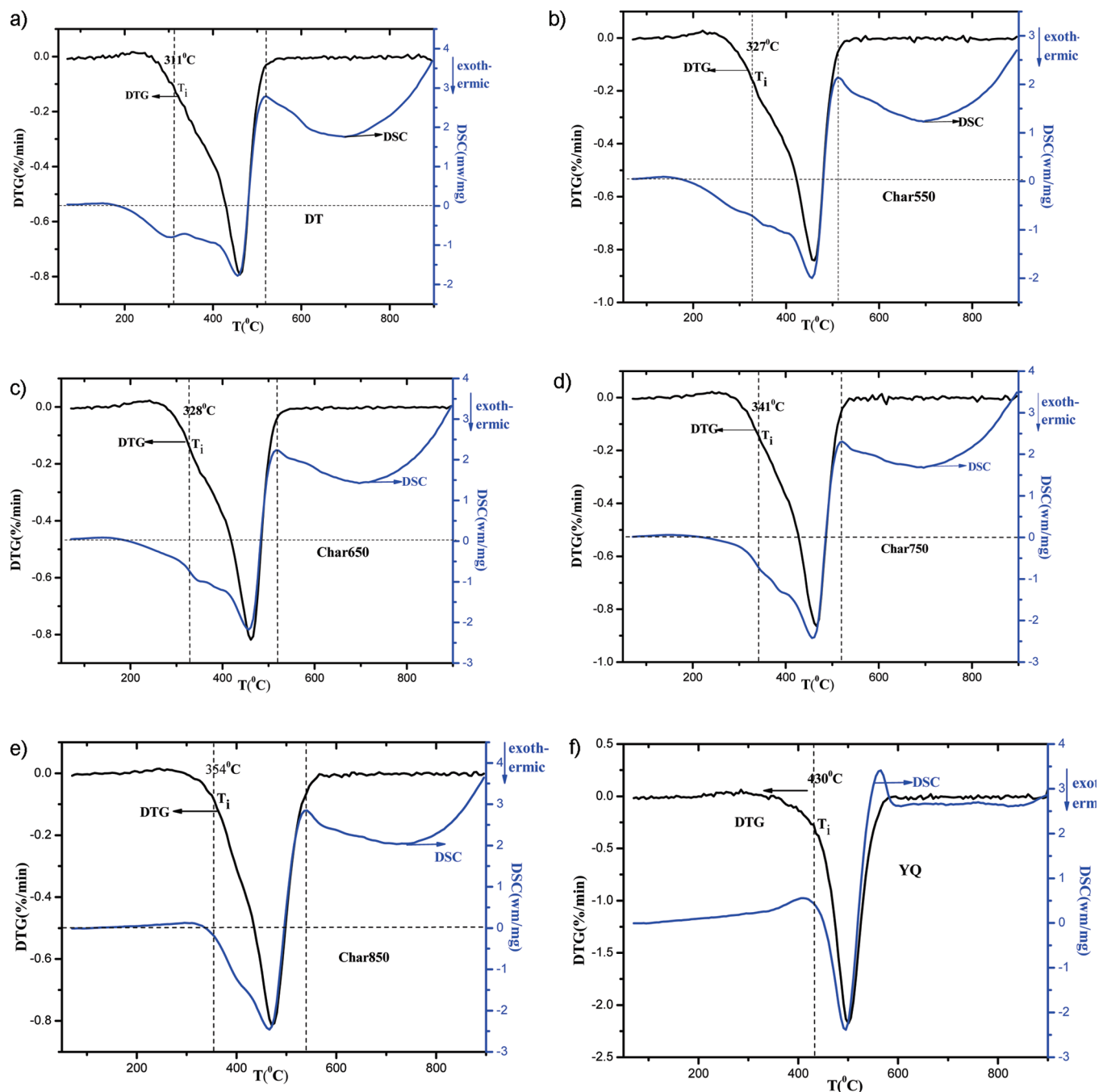


Figure 4. DSC and DTG curves of the coals and chars for the determination of ignition type.

Figure 6 shows the typical $\ln(1 - \alpha)^{-n} (d\alpha/dt)$ vs $1/T$ plots with different n values obtained from TG and DTG results of Char550. Figure 7 plots the relationship between $\ln(1 - \alpha)^{-n} (d\alpha/dt)$ vs $1/T$ with the n value of 2.8 for Char550. The combustion process of coal and chars is divided into four stages; each is classified based on the striking linearity of the $\ln(1 - \alpha)^{-n} (d\alpha/dt)$ vs $1/T$ plots in the region. The four stages represent (i) the initial ignition stage, (ii) the early combustion stage, (iii) the middle combustion stage, and (iv) the burnout stage. The apparent activation energy in each stage is calculated from eq 3; these are denoted as E_1 , E_2 , E_3 , and E_4 , respectively.

A weighted mean apparent activation energy (E_m), which was proposed by Cumming,³⁰ is used to rank the reactivity of coal and chars, when a defined experimental procedure is

rigidly followed. E_m is calculated by eq 4:

$$E_m = \sum_{i=1}^n E_i F_i \quad (4)$$

where F_1, \dots, F_n are the weight fractions of the combustible content of the samples burned in each region.

Figure 8 shows the E_m values, relative to different n values. Figure 9 presents the mean values of the linear correlation coefficients (R_i) of each stage and the mean value of R_i (R_a), relative to different n values. The parameters R_i and R_a are estimated by

$$R_i = \sum_{j=1}^6 \frac{R_{i,j}}{6} \quad (5)$$

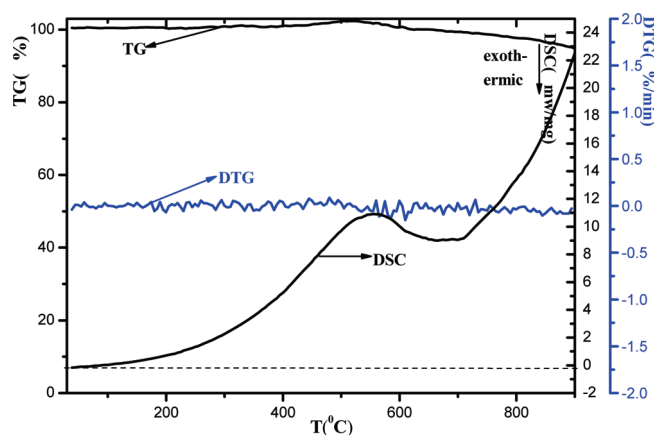


Figure 5. TG, DTG, and DSC curves of Char550 residual ash in an air atmosphere.

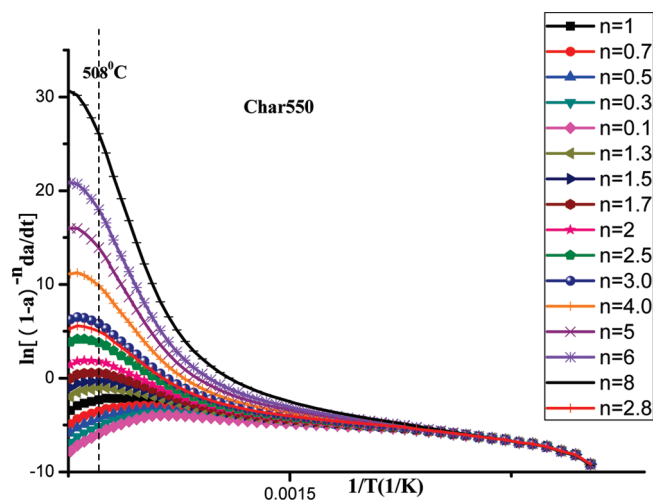


Figure 6. Typical $\ln(1 - \alpha)^{-n} (da/dt)$ vs $1/T$ plots for different n values.

$$R_a = \sum_{i=1}^4 \frac{R_i}{4} \quad (6)$$

where $R_{i,j}$ is the linear correlation coefficients of stage i of sample j (DT, Char550, Char650, Char750, Char850, YQ).

It is shown that the value of E_m increases as n increases for all samples. For the same n value, the order of E_m values are as follows: $E_{m,DT} < E_{m,Char650} < E_{m,Char550} < E_{m,Char850} < E_{m,Char750} < E_{m,YQ}$. Figure 9 reveals that R_a remains more or less the same as the n values vary. Table 4 summarizes the temperature regions, the fitted linear equation for each region, the linear correlation coefficients, E_i , F_i , and E_m for all chars and coals with $n = 2.8$.

3.4. Discussion of Char Reactivity and Affecting Factors. **3.4.1. Char Reactivity.** Tables 3 and 4 show that both the T_i and E_m values of all chars are higher than those of DT bituminous coal but lower than those of YQ anthracite. This indicates that the residual chars, derived from flash pyrolysis under relatively mild conditions, have lower reactivity than the parent coal but have higher reactivity than the anthracite. Thermal deactivation occurs for bituminous coal during pyrolysis. The increments of the T_i and E_m (ΔT_i and ΔE_m) values for the chars, in comparison with DT coal, are listed in Tables 3 and 4, respectively. It can be seen that the decrement of reactivity for Char550 and Char650 is small,

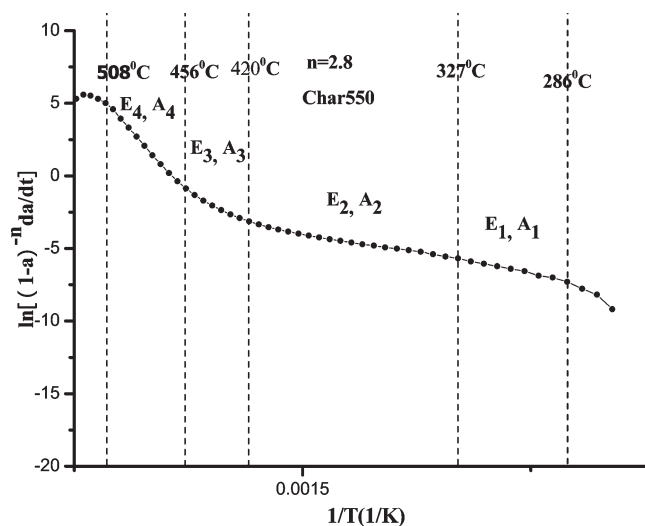


Figure 7. Typical $\ln(1 - \alpha)^{-n} (da/dt)$ vs $1/T$ plot for $n = 2.8$.

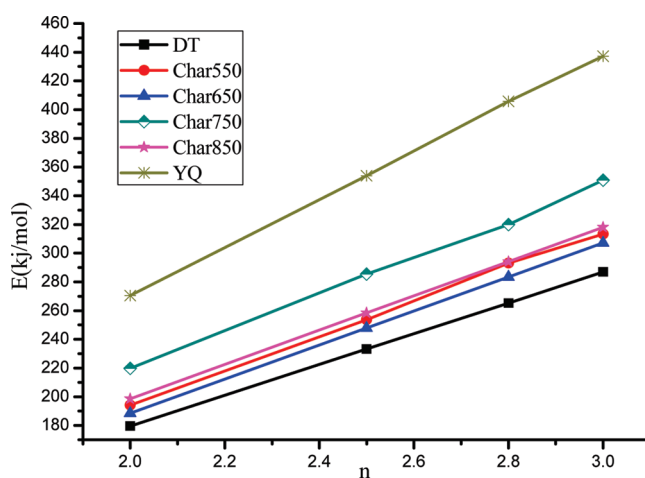


Figure 8. Values of weighted mean apparent activation energy (E_m), relative to different values of n .

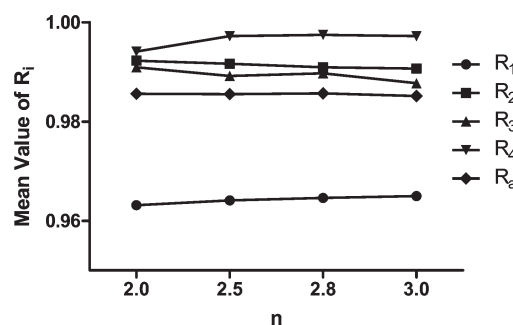


Figure 9. Mean value of linear correlation coefficients, relative to different values of n .

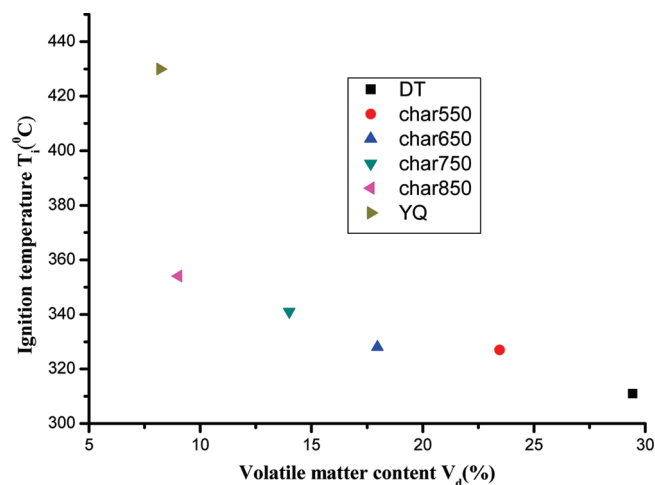
but that for Char750 and Char850 is relatively larger. Table 3 shows that the ignition temperature (T_i) of the chars increases as the pyrolysis temperature increases. However, the order of apparent activation energy of the chars is as follows: $E_{m,char650} < E_{m,char550} < E_{m,char850} < E_{m,char750}$.

3.4.2. Effect of Volatile Content on Reactivity. Figure 10 presents the relationship between the ignition temperature and volatile content. Figures 11 and 12 show the relationship between E_m and volatile content and that between

Table 4. Summaries of Apparent Activation Energies for Various Coals and Chars

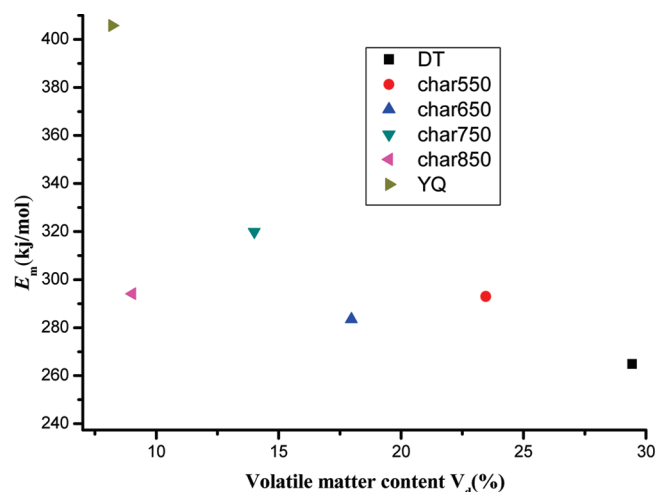
temperature range (°C)	fitting straight line	linear correlation coefficient	E_i (kJ/mol)	F_i
DT, $E_m = 264.89$ kJ/mol				
286–311	$Y = 10974.19221x + 12.80981$	0.99092	91.24	0.018
311–412	$Y = -9466.47x + 10.20803$	0.99647	78.71	0.302
412–442	$Y = -24005.1318x + 31.45629$	0.99017	199.60	0.253
442–506	$Y = -58731.2797x + 79.57992$	0.9977	488.32	0.387
Char550, $E_m = 293.04$ kJ/mol, $\Delta E_m = 28.15$ kJ/mol ^a				
286–327	$Y = -12868.8727x + 15.79769$	0.99451	107.00	0.04
327–420	$Y = -10163.2592x + 11.25251$	0.98978	84.50	0.336
420–456	$Y = -32185.1490x + 43.09376$	0.99144	267.60	0.315
456–508	$Y = -70123.6828x + 95.13735$	0.99913	583.04	0.302
Char650, $E_m = 283.46$ kJ/mol, $\Delta E_m = 18.57$ kJ/mol ^a				
306–328	$Y = -14119.7460x + 17.72847$	0.99345	117.40	0.023
328–421	$Y = -9973.79073x + 10.8285$	0.98965	82.93	0.32
421–452	$Y = -28951.7165x + 38.32784$	0.9878	240.72	0.261
456–508	$Y = -61383.87069x + 82.9548$	0.99607	510.38	0.375
Char750, $E_m = 319.94$ kJ/mol, $\Delta E_m = 55.05$ kJ/mol ^a				
306–341	$Y = -15418.0018x + 19.39124$	0.99054	128.19	0.036
341–426	$Y = -11783.8503x + 13.36964$	0.99003	97.98	0.327
426–462	$Y = -35002.5978x + 46.52068$	0.98925	291.03	0.302
462–517	$Y = -71428.8669x + 95.92661$	0.99576	593.90	0.329
Char850, $E_m = 294.17$ kJ/mol, $\Delta E_m = 29.28$ kJ/mol ^a				
325–354	$Y = -20268.9584x + 26.24727$	0.99244	168.53	0.011
354–436	$Y = -14651.1854x + 17.12791$	0.99807	121.82	0.301
436–462	$Y = -29564.2010x + 38.12747$	0.99293	245.81	0.200
462–540	$Y = -53063.530x + 69.88894$	0.99831	441.20	0.468
YQ, $E_m = 405.71$				
380–410	$Y = -10690.3125x + 10.05551$	0.82695	88.89	0.019
410–446	$Y = -17293.6892x + 19.75022$	0.98092	143.79	0.107
446–485	$Y = -35070.1414x + 44.13839$	0.9916	291.59	0.223
485–560	$Y = -62675.5254x + 80.21649$	0.99792	521.12	0.621

$$^a \Delta E_m = E_{m, \text{char}} - E_{m, \text{DT}}$$

**Figure 10.** Relationship between ignition temperature and volatile content.

E_m and fuel ratio (ratio of fixed carbon to volatile matter), respectively.

The T_i value of the samples decreases as the volatile content increases, indicating that the difference in ignitability between DT bituminous coal and its chars is mainly caused by the decreasing volatile content when increasing the pyrolysis temperature. Su et al.³² reviewed three scales of

**Figure 11.** Relationship between E_m and volatile content.

tests and determined that volatile content is a common index in predicting the ignitability of coal/blends. Ignitability seems to improve with increasing volatile matter of coal/blends, except for low-rank coals. Our results are consistent with those of Su et al.³²

The values of the apparent activation energies seem to follow the trend that E_m decreases as the volatile content increases and increases as the fuel ratio increases. However, an exception exists; for example, the E_m value of Char650 is lower than that of Char550, although Char650 has a lower volatile content and higher fuel ratio than Char550.

(32) Su, S.; Pohl, J. H.; Holcombe, D.; Hart, J. A. Techniques to determine ignition, flame stability and burnout of blended coals in p.f. power station boilers. *Prog. Energy Combust. Sci.* **2001**, 27 (1), 75–98.

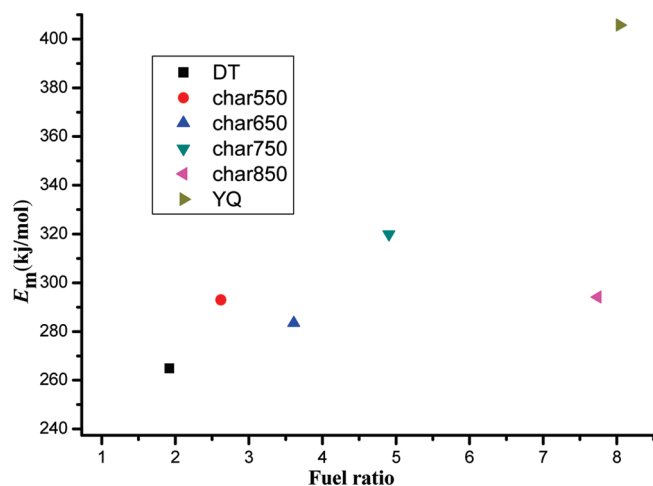


Figure 12. Relationship between E_m and fuel ratio.

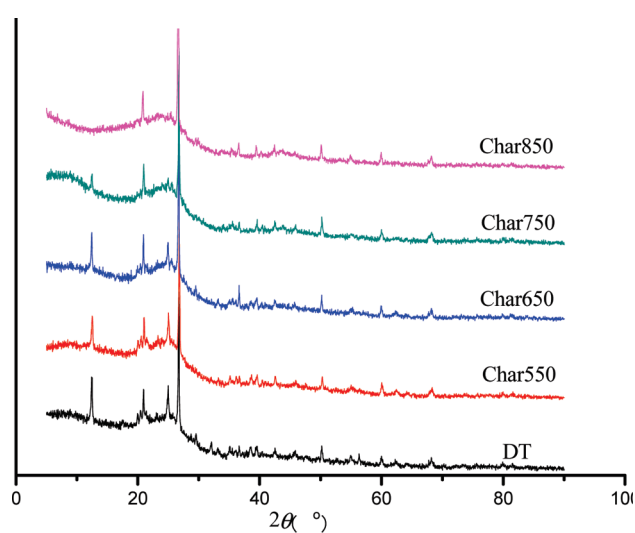


Figure 13. XRD spectrum of DT coal and its chars derived at different temperatures.

3.4.3. Effect of Carbon Structure Ordering on Reactivity.

Figure 13 presents the XRD spectrum of DT bituminous coal and its chars. XRD measurement provides information regarding char crystallinity. In the XRD spectra, carbonaceous materials produce two broad peaks: the (002) and the (10) planes of the carbon crystal lattice at $2\theta \approx 25^\circ$ and 44° . Those correspond to the stacking height and radial spread of crystalline structures, respectively. Figure 13 shows that no significant change occurs in the XRD spectrum of Char550 and Char650, compared to that of DT coal. This indicates that carbon structure ordering is not obvious at pyrolysis temperatures of 550 and 650 °C. However, for Char750 and Char850, the (002) peak (near the point where $2\theta \approx 25^\circ$) becomes more clear than that for the parent coal, especially for Char850. Two broad peaks in the XRD spectrum of Char850 indicate that carbon structure ordering is evident.

From the aforementioned analysis, it seems that the reactivity decrement of Char550 and Char650 may not be caused by carbon structure ordering. However, for Char750

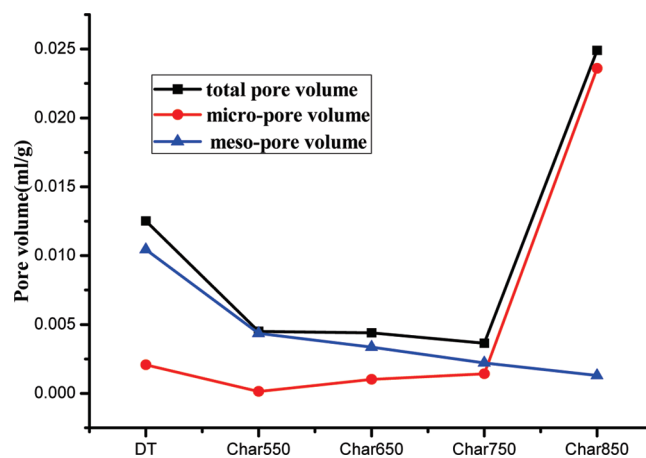


Figure 14. Pore volume of DT coal and chars.

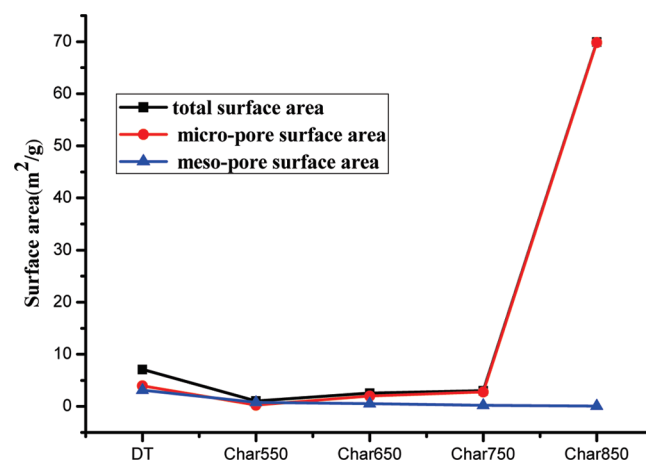


Figure 15. Pore surface area of DT coal and chars.

and Char850, carbon structure ordering may contribute to thermal deactivation, to a certain degree.

3.4.4. Effect of Pore Structure on Reactivity. According to previous studies,^{33,34} the pore structure evolution of coal particles during pyrolysis is mainly dependent on the following factors: the thermoplastic properties of coal particles; volatile release during pyrolysis; and surface tension, which is caused by thermoplastic deformation. Previous studies concluded that, during the pyrolysis process, plastic coal particles swell to different extents and therefore generate solid residues with different physical structures.³³ During the swelling process, the surface tension of the particles may cause the original pore to close or become smaller.³⁴ Volatile release can produce new micropores and enlarge original pores or make original pores combine with neighboring pores.³⁴

The total pore volume, the mesopore ($2 \text{ nm} < d < 50 \text{ nm}$) volume, and the micropore ($d < 2 \text{ nm}$) volume for DT bituminous coal and its chars are shown in Figure 14. The total surface area, mesopore surface area, and micropore surface area are given in Figure 15.

Figure 14 shows that the mesopore volume decreases as the pyrolysis temperature increases; the micropore volume decreases in ranking from DT bituminous to Char550, then it

(33) Yu, J.; Lucas, J. A.; Wall, T. F. Formation of the structure of chars during devolatilization of pulverized coal and its thermoproperties: A review. *Prog. Energy Combust. Sci.* **2007**, *33* (2), 135–170.

(34) Qiu, J. H. Variation of surface area and pore structure of pulverized coal during pyrolysis. *J. Fuel Chem. Technol.* **1994**, *22* (3), 316–320.

increases slightly as the pyrolysis temperature increases before 750 °C and it increases drastically at 850 °C. The total pore volume decreases as the pyrolysis temperature increases before 750 °C. The change trend is the same as that of the mesopore volume before 750 °C. However, the total pore volume increases suddenly when the pyrolysis temperature reaches to 850 °C. That is because the micropore volume increases drastically at 850 °C. This suggests that the change of pore volume, to a large extent, is dependent on the variation of mesopores.

Figure 15 shows that the mesopore surface area decreases as the pyrolysis temperature increases, which is consistent with the change in mesopore volume. The micropore surface area decreases from DT bituminous to Char550, and then increases slightly as the pyrolysis temperature increases before 750 °C. At 850 °C, the micropore surface area increases drastically. The change trend of the micropore surface area is consistent with that of the micropore volume. The total surface area has the same change trend as that of the micropore surface area, which implies that the change in surface area is dependent, to a large extent, on the variation of micropores.

The pore structure of a char plays a significant role in its reactivity during char oxidation.³⁵ The total pore volume influences the transport characteristics of the reacting gases inside the sample particles, and the total surface area affects the size of the effective surface area that may be accessible to the reacting gases. Both the total pore volume and the pore surface area of Char850 are the highest, and its surface area is much greater than that of the other three chars. Therefore, the E_m value of Char850 is not the highest among all chars (see Table 4), although it has the lowest V_d value and the highest fuel ratio (see Table 2) among the four chars. Char650 has almost the same total pore volume (0.0044 mL/g) as Char550 (0.0045 mL/g), but the total surface area of Char650 (2.537 m²/g) is larger than that of Char550 (1.043 m²/g), and the differences in V_d , and the fuel ratio between Char550 and Char650, are not large (see Table 2). Therefore, the E_m value of Char650 is slight less than that of Char550. Although Char550 has the lowest total surface area among the chars, it has a larger total pore volume than that of Char750; moreover, it has the lowest fuel ratio and the highest V_d value among the chars, so the E_m value of Char550 is less than that of Char750. Compared to Char550

and Char650, Char750 has medial-level pore structures but a higher fuel ratio and a lower V_d value, so it has the highest E_m . These indicate that E_m cannot be determined by one factor.

4. Conclusions

Bituminous chars were pyrolyzed at four different temperatures (550, 650, 750, and 850 °C). The ignition temperature and combustion reactivity of the chars, the parent coal, and an anthracite (Yangquan anthracite, YQ) were determined by simultaneous thermal analysis (STA). From this study, the following conclusions can be drawn.

(1) Both the ignition temperature (T_i) and the apparent activation energy (E_m) of the chars are higher than those of Datung (DT) bituminous coal but lower than those of YQ anthracite. This indicates that the chars have lower reactivity than DT bituminous coal and higher reactivity than YQ anthracite. That is, thermal deactivation phenomena exist even at low pyrolysis temperatures, such as 550 and 650 °C. The ignition type is hetero-homogeneous for the parent coal, Char550, Char650, and Char750, and it is heterogeneous for Char850 and YQ anthracite.

(2) Compared to the parent coal, the decrement in reactivity for Char550 and Char650 is small, especially for Char650. It is slightly higher for Char750 and Char850. The T_i value of the chars increases as the pyrolysis temperature increases. The size of the E_m values of the chars is ranked in the following order: $E_{m,char650} < E_{m,char550} < E_{m,char850} < E_{m,char750}$.

(3) Carbon structure ordering does not seem to be the cause of thermal deactivation at low pyrolysis temperatures (550 °C, 650 °C). However, it does seem to have an important contribution to thermal deactivation at high pyrolysis temperatures (750 °C, 850 °C). The changes in pore structure and material composition affect the reactivity of both low-temperature char and high-temperature char. The char reactivity needs to be determined by combination of these parameters instead of using one of them.

(4) Taking both T_i and E_m into consideration, Char650 has the highest reactivity among the chars.

(5) It seems possible that chars derived from the coal topping process may be used as fuels for the pulverized coal combustion boiler.

Acknowledgment. This work was sponsored by the Hi-Tech Research and Development Program of China (863 Program), under Contract No. 2006AA05Z312, and the Science Foundation of the Chinese Academy of Sciences, under Contract No. 20221603.

(35) Liu, G. S. *Mathematical Modelling of Coal Char Reactivity in a Pressurised Entrained Flow Gasifier*, Ph.D. Thesis, University of Newcastle—Australia, 1999.